Forty-Eighth Annual Allerton Conference
Allerton House, UIUC, Illinois, USA
September 29 - October 1, 2010

Load-shedding probabilities with hybrid renewable power generation and energy storage

Huan Xu, Ufuk Topcu, Steven H. Low, Christopher R. Clarke, and K. Mani Chandy

Abstract— **The integration of renewable energy resources, such as solar and wind power, into the electric grid presents challengs partly due to the intermittency in the power output. These difficulties can be alleviated by effectively utilizing energy storage. We consider, as a case study, the integration of renewable resources into the electric power generation portfolio of an island off the coast of Southern California, Santa Catalina Island, and investigate the feasibility of replacing diesel generation entirely with solar photovoltaics (PV) and wind turbines, supplemented with energy storage. We use a simple storage model alongside a combination of renewables and varying load-shedding characterizations to determine the appropriate area of PV cells, number of wind turbines, and energy storage capacity needed to stay below a certain threshold probability for load-shedding over a pre-specified period of time and long-term expected fraction of time at load-shedding.**

I. Introduction

Santa Catalina Island is 26 miles off the coast of Southern California, USA. It is 21 miles long and 76 square miles in area with 54 miles of coastline. The island's population in the 2000 census was 3,696 with 90 percent living in the two largest cities Avalon and Two Harbors [1]. Catalina is served by three 12kV distribution circuits that are separate from the grid on the mainland of California with a peak demand in 2008 of 5.7MW [2]. Currently, electricity is generated from a central diesel plant. It is desirable to reduce diesel-based generation for several reasons (both environmental and economical): to reduce the emissions from diesel power plants and to eliminate the cost of transportation of diesel fuel to the island. Furthermore, the diesel generators are most efficient when running at full capacity and are therefore inefficient for Santa Catalina Island, where the daily demand peaks for a relatively short period of time. This paper aims to asses the feasibility of replacing diesel generation with generation from intermittent renewable resources (e.g., solar, wave, and wind power generation).

Fluctuation in both the generation and demand as well as physical distance between generation sites and users make the integration of renewable sources into the electricity grid difficult [3], [4]. The potential benefits, however, can be utilized by supplementing the system with energy storage [5], [6]. Different techniques have been used in determining the correct sizing for storage needed in the presence of intermittent renewable sources as a function of storage efficiency, conventional fossil fuel generation and life cycle costs [7], [8], [9]. Reference [10] uses a probabilistic model to predict the feasibility of increased renewable penetration by investigating different types, sizes, and time scales of storage technologies. References [11] and [12] examine the integration of wind power into isolated systems, similar to Catalina Island.

H. Xu, U. Topcu, S. H. Low, and K. M. Chandy are with California Institute of Technology. E-mails addresses: mumu@caltech.edu, utopcu@cds.caltech.edu, slow@caltech.edu, mani@cs.caltech.edu. C. R. Clarke is with Southern California Edison. E-mail address: Christopher.R.Clarke@sce.com.

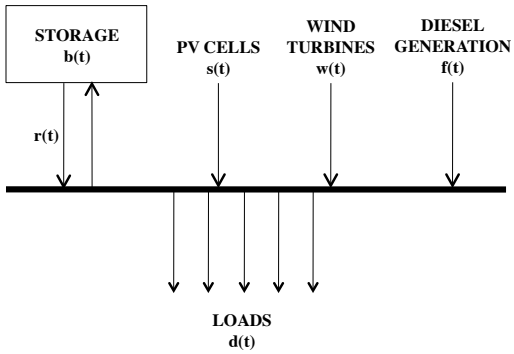

Fig. 1. A schematic for a power network with renewable sources. Demand loads are met by base diesel generation, supplemented with PV cells, wind turbines, and energy storage.

In this paper, we incorporate simple storage dynamics into a load-shedding model to understand the effects of intermittency in generation and/or demand on the characteristics of the electricity network. We consider a scenario where the electricity is supplied by a combination of solar photovoltaic (PV) cells, wind turbines, and base diesel generation. With these resources, we address the following design questions: Given information about typical demand and generation profiles over certain periods of time, what are the appropriate amounts of each resource and energy storage capacity needed to ensure a certain level of reliable operation [13], e.g., that the probability of load-shedding is smaller than a pre-specified threshold and the long-term expected fraction of time spent at load-shedding is sufficiently small?

II. Set up and problem formulation

A. Simple storage model

Consider the configuration in Figure 1. In this figure and hereafter, $d(t)$ denotes the total amount of all loads over the time period $[t, t+1]$. Additionally, $s(t), w(t)$, and $f(t)$ denote the amount of energy generation by a unit area of PV cells, a wind turbine, and diesel (fossil fuel) based generators over $[t, t+1]$. The amount of energy storage at time t is denoted by $b(t)$ and is considered to follow the first order difference

equation

$$b(t+1) = b(t) + g(t) - d(t), \text{ for } t = 0, \ldots, T-1 \quad (1)$$

with the initial amount $b(0)$ of storage and the length T of the time horizon. Total generation $g(t)$ is defined as

$$g(t) := \gamma_1 s(t) + \gamma_2 w(t) + f(t),$$

where γ_1 and γ_2 are the numbers of unit area of PV cells and wind turbines in the system. Additionally, the following non-negativity and capacity constraints on the amount of storage are imposed

$$0 \leq b(t) \leq B, \text{ for } t = 1, \ldots, T,$$

where B denotes the storage capacity.

At time $t+1$, we call the case in which the difference between demand and total generation is strictly less than the available stored energy, i.e.,

$$b(t) < -g(t) + d(t), \quad (2)$$

as load-shedding.

B. Problem description

In general, the load d and renewable generation s and w feature intermittency and fluctuations [10]. For example, consider the daily d, s, and w profiles shown in Figure 2, which are also used in the analysis in the subsequent sections. Each of the figures show d, s, and w at each hour for 31 days in the month December 2009 obtained at geographical locations with characteristics similar to those of Santa Catalina Island (discussed at the end of this section). The load and solar graphs follow a profile with considerable fluctuations, while the wind profile is even less predictable.

In the face of stochasticity in both loads and generation, we are interested in quantifying the probability of having load-shedding and the effects of energy storage on this probability in configurations with different levels of intermittent renewable and diesel-based generation. Note that, in general, the likelihood of load-shedding is a function of the generation and demand profiles and, therefore, it is a function of γ_1, γ_2, and B (potentially along with other factors not modeled here). The total area of PV cells, number of wind turbines, and capacity of storage are design-time decisions to be made before investing in the deployment of large renewable energy generation and accompanying energy storage. In the following, we consider the question of determining appropriate values for γ_1, γ_2, and B that lead to an acceptable probability of load-shedding.

C. Description of data set

In this study, we use a data set including load (d), solar generation (s), and wind generation (w) obtained in the following way.

- Load profile: Only peak demand values are available for Santa Catalina Island[1]. Therefore, load profiles are generated from a proxy distribution circuit statistically similar to that for the island, e.g., line distances, customer count, and climate. The proxy circuit peak is scaled to match the peak data for each of the three distribution circuits on the island. Hourly averages calculated for times where more than one data point was available, while data for missing hours are interpolated.
- Solar generation profile: Hourly data are obtained using the Solar Advisor Model (a detailed performance model for solar technologies - available at `https://www.nrel.gov/analysis/sam/`) with Long Beach, California as a geographic location and each PV cell unit measuring 35 m^2.
- Wind generation profile: Hourly data is obtained from the National Renewable Energy Laboratory (NREL) website available at `http://wind.nrel.gov/Web_nrel/` for a station located off an island near Santa Barbara, California.

[1]These peak values are obtained through personal communication with researchers from Southern California Edison

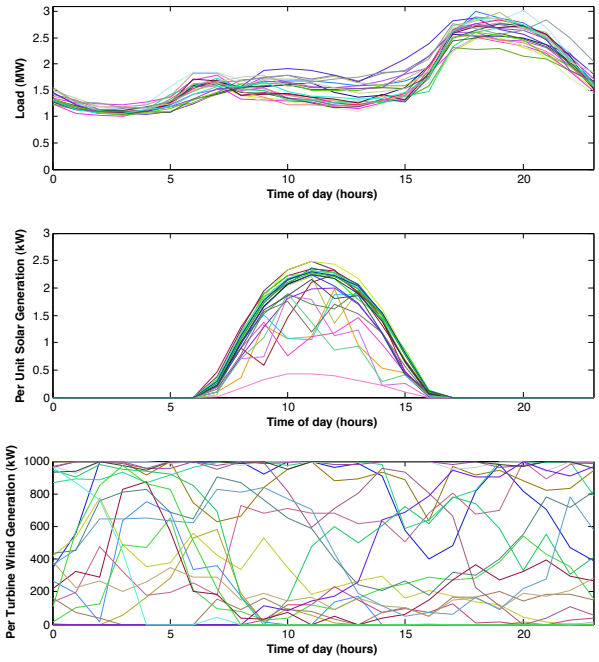

Fig. 2. Daily load profiles on Santa Catalina Island (top), solar generation profiles in Long Beach, CA (middle), and wind generation profiles on an island near Santa Barbara, CA (bottom), for the month of December.

III. Probability of load-shedding

In this section, we investigate the effects of varying amounts of renewable generation (i.e., γ_1 and γ_2) and storage capacity (B) on the probability of load-shedding over the time horizon $t = 1, \ldots, T$ defined as

$$P_{LS} := \textbf{Prob}[b(t) < -g(t) + d(t) \text{ for some } t \in \{0, 1, \ldots, T-1\}].$$

A. Estimating the probability of load-shedding

In order to estimate the load-shedding probability, we quantize the allowable range $[0, B]$ of energy storage using n equally spaced points $\beta_1 = B > \beta_2 > \cdots > \beta_{n-1} > \beta_n = 0$ and

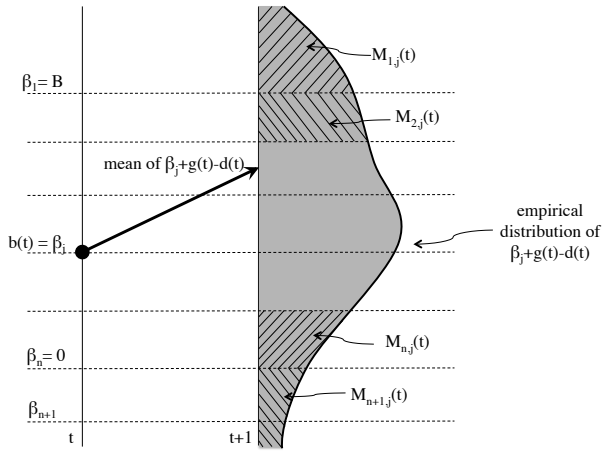

Fig. 3. Construction of matrix $M_{i,j}(t)$ is based on the empirical distribution for $g(t)-d(t)$.

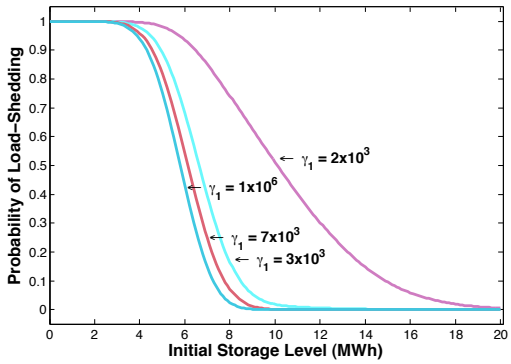

Fig. 4. Probability of load-shedding versus amount of initial energy storage with $B = 20$ MWh, $T = 24$ hours, and $\gamma_2 = 1$ (i.e., a single wind turbine), for different levels of solar generation.

assigning β_{n+1} as the state corresponding to load-shedding. For $i, j = 1, \ldots, n+1$ and time $t = 0, \ldots, T-1$, define

$$M_{i,j}(t) := \textbf{Prob}[b(t+1) = \beta_i \mid b(t) = \beta_j]$$

as the probability of having a storage level of β_i at time $t+1$ given that the storage level B is β_j at time t. Using the data shown in Figure 2, we empirically estimate $M_{i,j}(t)$ for $t = 0, \ldots, T-1$ as follows. Define the intervals

$$\begin{aligned} I_1 &:= [\beta_1 = B, \infty), \\ I_i &:= [\beta_i, \beta_{i-1}), \text{ for } i = 2, \ldots, n, \\ I_{n+1} &:= (-\infty, \beta_n = 0). \end{aligned}$$

Then, for $t = 0, \ldots, T-1$, $j = 1, \ldots, n$, and $i = 1, \ldots, n+1$, an empirical estimate of $M_{i,j}(t)$ is the fraction of points in the set of data points $\beta_j + g(t) - d(t)$ that fall in I_i with the convention $M_{n+1,n+1}(t) = 1$ and $M_{i,n+1}(t) = 0$ for $i = 1, \ldots, n$. Note that β_{n+1} is an absorbing state of the Markov chain governed by the matrix $M(t)$ [14].

Define

$$\mathbf{M} := M(T-1)M(T-2)\ldots M(0).$$

Then, the probability

$$\begin{aligned} &\textbf{Prob}[b(t) < -g(t) + d(t) \\ &\qquad \text{for some } t \in \{0, \ldots, T-1\} \mid b(0) = \beta_j] \end{aligned}$$

of transitioning to the load-shedding state β_{n+1} at some time $t = 1, \ldots, T$ from $b(0) = \beta_j$ is estimated by $\mathbf{M}_{n+1,j}$.

B. Results

In this section, we discuss the results obtained for $T = 24$ hours and storage capacity $B = 20$ MWh using the hourly load, solar generation, and wind generation profiles in Figure 2. A quantization increment of $\beta_{j-1} - \beta_j = 100$ kWh for $i = 2, \ldots, n$ over $[0, B]$ is used.

Figure 4 shows the load-shedding probabilities versus initial storage levels for different levels of solar generation with $\gamma_2 = 1$ (i.e., a single wind turbine), and without any base diesel generation (i.e., $w(t) = 0$ and $f(t) = 0$ for $t = [0, T]$). Note the transition from high P_{LS} at low levels of initial energy storage to low P_{LS} at higher levels of initial energy storage. There are at least two trends in Figure 4 that are of interest.

- As the level of solar generation increases, (i.e., γ_1 increases), the amount of initial storage at which the transition from high P_{LS} to low P_{LS} decreases and approaches a constant value which can be attributed to the mismatch between the generation and demand at the beginning of the day due to lack of any solar generation.
- As γ_1 increases, the transition from high P_{LS} to low P_{LS} sharpens. This can be attributed to the higher variability in wind generation compared to that in solar generation (see Figure 2).

Figure 5 shows the load-shedding probabilities versus initial amount of storage with a fixed level of solar generation $\gamma_1 = 2 \cdot 10^3$ for different number γ_2 of wind turbines. Similar to the trend with increasing γ_1 in Figure 4, the level of initial storage at which the transition from high P_{LS} to low P_{LS} occurs decreases with increasing γ_2. Unlike the trends for increasing γ_1, P_{LS} can be made less than one even for zero initial storage with sufficiently large γ_2 (e.g., $\gamma_2 = 5$ in Figure 5).

In the results shown in Figures 4 and 5, the base diesel generation is considered to be zero. We now include base generation and investigate the probability of load-shedding as a function of the level of penetration of renewable energy resources. Assuming that the base generation P_B is constant over time, we define the penetration ratio ρ as

$$\rho := \frac{P_R}{P_R + P_B},$$

where P_R is the largest value of renewable generation over a pre-specified time window of interest. For ease of presentation, we consider that solar generation is the only renewable resource, and take P_R as γ_1 times the largest value of solar generation in the data set shown in Figure 2 (middle). Then, ρ is a function of γ_1 and P_B. Figure 5 shows P_{LS} versus initial

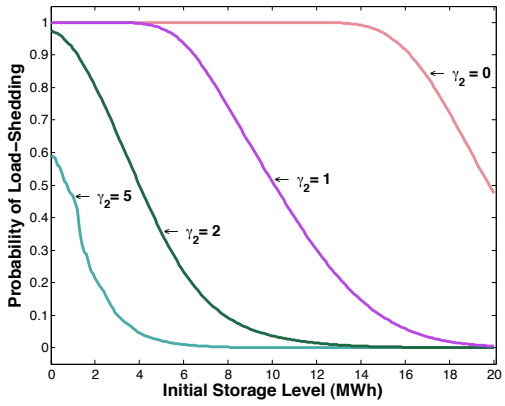

Fig. 5. Probability of load-shedding versus amount of initial energy storage with $B = 20$ MWh, $T = 24$ hours, and fixed $\gamma_1 = 2 \cdot 10^3$ for different values of γ_2 (i.e., number of wind turbines).

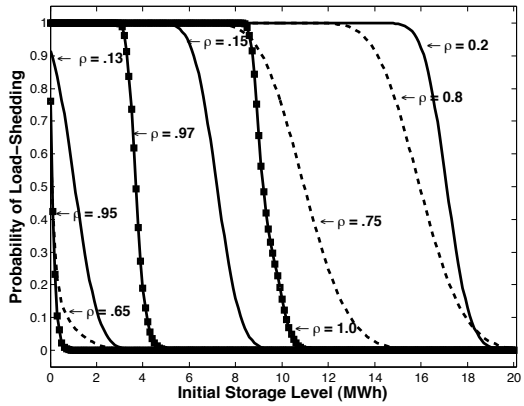

Fig. 6. The probability of load-shedding versus initial amount of storage with $B = 20$ MWh and $\gamma_2 = 0$ for different penetration levels ρ. $\gamma_1 = 10^2$ (solid curves), $\gamma_1 = 10^3$ (dashed curves), $\gamma_1 = 10^4$ (solid curves with square markers).

amount of storage with $\gamma_2 = 0$ for different penetration levels ρ.

IV. Long-term duration of load-shedding and energy not-served

The simple load-shedding characterization discussed in Section III does not distinguish between levels of load-shedding by using a single lumped state β_{n+1} corresponding to the condition $b(t) < -g(t) + d(t)$. In this section, we modify the load-shedding characterization to allow multiple levels of deficit $d(t) - g(t) - b(t)$. This characterization allows us to estimate the (long-term) expected time spent at a load-shedding state and expected amount of energy not-served. To this end, let $\beta_1 = B > \beta_2 > \cdots > \beta_{n-1} > \beta_n = 0$ be equally spaced points over $[0, B]$ as before and $\beta_{n+1}, \ldots, \beta_{n+m}$ be such that $\beta_n = 0 > \beta_{n+1} > \cdots > \beta_{n+m}$. Consider that the amount of energy storage evolves by following the difference

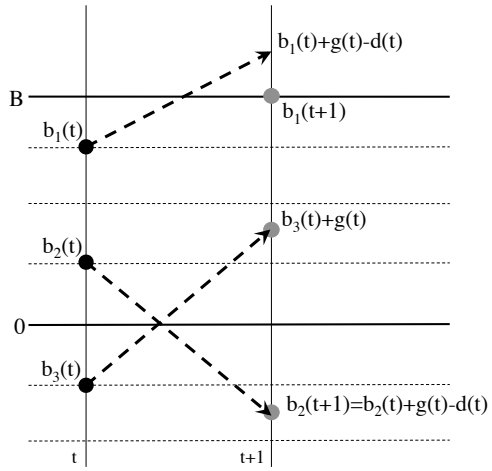

Fig. 7. Transitions governed by (3) for three different values of storage at time t.

equations

$$b(t+1) = b(t) + g(t) - d(t) \text{ if } b(t) \geq 0$$
$$b(t+1) = b(t) + g(t) \text{ if } b(t) < 0 \quad (3)$$

with saturation at β_{n+m} and B. Figure 7 depicts the transitions for three different values of "storage" at time t.

Note that, in (3), a negative value for $b(t)$ is used to quantify the severity of load-shedding and $\beta_{n+1}, \ldots, \beta_{n+m} < 0$ correspond to different levels of load-shedding. With potential abuse of terminology, we do not distinguish between $b(t) \geq 0$ and $b(t) < 0$ and refer to both as the *amount of storage*. The transitions from storage levels $\beta_j \geq 0$ and $\beta_j < 0$ are different. If the storage level $b(t) = \beta_j < 0$, then generated energy is used to reduce the severity of load-shedding.

We again empirically estimate the probability $M_{i,j}(t)$ of having $b(t+1) = \beta_i$ given that $b(t) = \beta_j$ for $t = 0, \ldots, T-1$. To this end, define

$$I_1 := [\beta_1 = B, \infty),$$
$$I_i := [\beta_i, \beta_{i-1}), \quad i = 2, \ldots, n+m-1,$$
$$I_{n+m} := (-\infty, \beta_{n+m-1}).$$

Then, an empirical estimate of $M_{i,j}(t)$ is the fraction of points in the set of points

- $\beta_j + g(t) - d(t)$ that fall in I_i for $i = 1, \ldots, n+m$ and $j = 1, \ldots, n$
- $\beta_j + g(t)$ that fall in I_i for $i = 1, \ldots, n+m$ and $j = n+1, \ldots, n+m$.

Define

$$\mathbf{M} := M(T-1)M(T-2)\ldots M(0).$$

In the case where $\mathbf{M}$ has a unique eigenvalue at 1 with $\mathbf{M}\pi = \pi$, $\pi_i \geq 0$ for $i = 1, \ldots, n+m$ and $\pi_1 + \cdots + \pi_{n+m} = 1$, π is called the stationary distribution for the Markov chain induced by $\mathbf{M}$ and the $i-$th entry π_i of π can be interpreted as the long-term expected fraction of time $b(t)$ spends at state β_i (regardless of the initial conditions) at times $t = 0, T, 2T, \ldots$

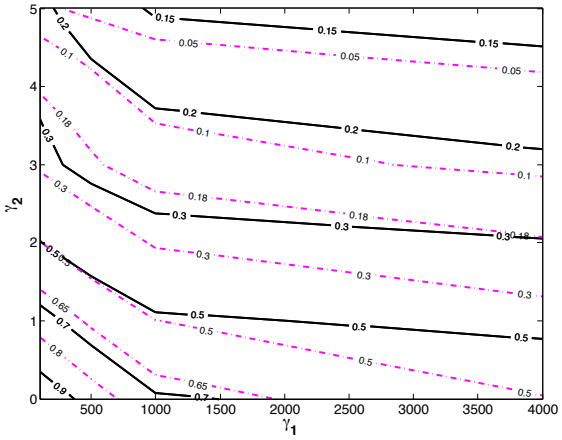

Fig. 8. The long-term expected fraction of time spent at a load-shedding state as a function of solar γ_1 and γ_2 for a storage capacities of $B = 3$ MWh (solid) and $B = 10$ MWh (dash-dot).

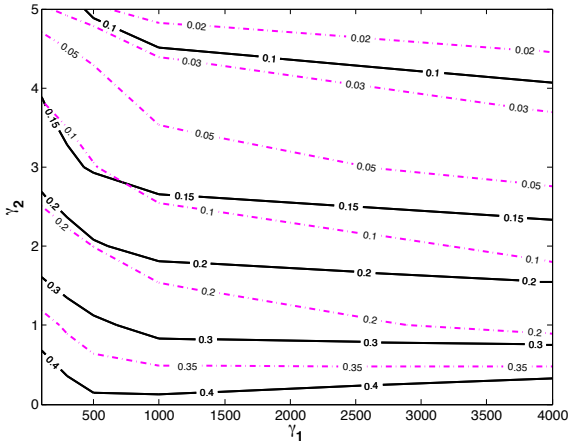

Fig. 9. The long-term expected energy not-served due to load-shedding normalized by the expected (normalized) total demand as a function of γ_1 and γ_2, for $B = 3$ MWh (solid) and $B = 10$ MWh (dash-dot).

[14], [15]. Let π be the stationary distribution for $\mathbf{M}$ (if it exists) and define

$$p(t) := M(t-1)\dots M(0)\pi, \quad t = 0,\dots,T-1.$$

Then, the long-term expected fraction of time spent at a load-shedding state can be estimated as

$$\frac{1}{T}\sum_{t=0}^{T-1}\sum_{i=n+1}^{n+m} p_i(t).$$

The long-term expected (normalized) energy not-served over the period $[0,T]$ due to load-shedding can be estimated as

$$\frac{1}{T}\sum_{t=0}^{T-1}\sum_{i=n+1}^{n+m} |\beta_i| p_i(t).$$

Figure 8 shows the long-term expected fraction of time spent at a load-shedding state with two different storage capacities $B = 3$MWh (solid, black curves) and $B = 10$MWh (dash-dot, magenta curves) for varying values of solar (i.e., γ_1) and wind (i.e., γ_2) generation. Figure 9 shows the ratio of the long-term expected normalized energy not-served due to load-shedding over a day to the expected total demand (load), i.e., mean of $\frac{1}{T}\sum_{t=0}^{T-1} d(t)$, as a function of γ_1 and γ_2 for $B = 3$ MWh (solid) and $B = 10$ MWh (dash-dot). Both quantities decrease with increasing levels of generation with fixed storage capacity and with increasing storage capacity for fixed γ_1 and γ_2. Figure 10 shows the effect of penetration ρ of renewable generation (as a function of the level of solar generation – with no wind generation) on the long-term expected fraction of time spent at a load-shedding state. Note three trends in the expected fraction of time at load-shedding:

- it increases with increasing penetration;
- for fixed ρ, it is smaller with $B = 10$ MWh compared to that with $B = 3$ MWh; and
- the down-shifting effect reduces with the decrease in the penetration level.

This final observation suggests that the amount of storage capacity will affect the tolerable level of penetration of renewable generation.

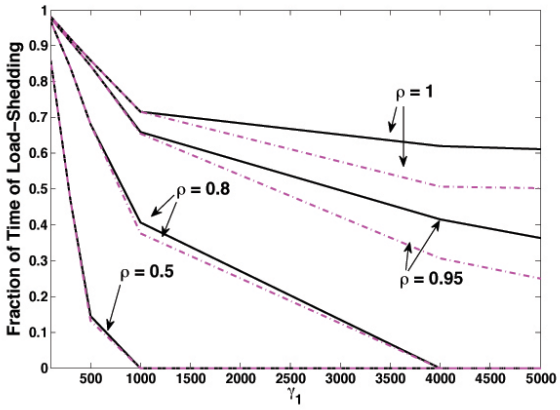

Fig. 10. The long-term expected fraction of time spent at a load-shedding state as a function of γ_1 (with $\gamma_2 = 0$) for varying levels ρ of penetration of renewable generation for two different storage capacities $B = 3$ MWh (solid) and $B = 10$ MWh (dash-dot). The curves for $\rho = 0.5$ are indistinguishable.

V. Effects of storage efficiency

Let us re-write the evolution of the amount of storage as

$$b(t+1) = b(t) + e(t), \quad \text{for } t = 0,\dots,T-1, \qquad (4)$$

where $e(t)$ denotes the amount of energy flow into the storage over $[t,t+1]$ if $e(t) \geq 0$ and the amount of energy flow out from the storage if $e(t) \leq 0$. Let $0 < \varepsilon_i \leq 1$ denote the efficiency of energy in-flow and $0 < \varepsilon_o \leq 1$ the efficiency of energy out-flow. In order to investigate the effects of the efficiency of charging and discharging, let us modify (4) as

$$b(t+1) = b(t) + \min\left\{\varepsilon_i e(t), \frac{1}{\varepsilon_o} e(t)\right\}. \qquad (5)$$

Define the overall efficiency of storage as $\varepsilon := \varepsilon_i \varepsilon_o$. Figure 11 shows the probability of load-shedding over 24 hours versus

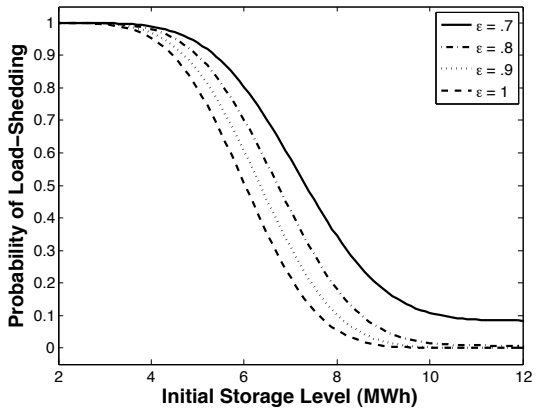

Fig. 11. Probability of load-shedding versus amount of initial storage with $B = 20$MWh, $\gamma_1 = 10^4$, $\gamma_2 = 1$, and $T = 24$ hours for varying values of ε.

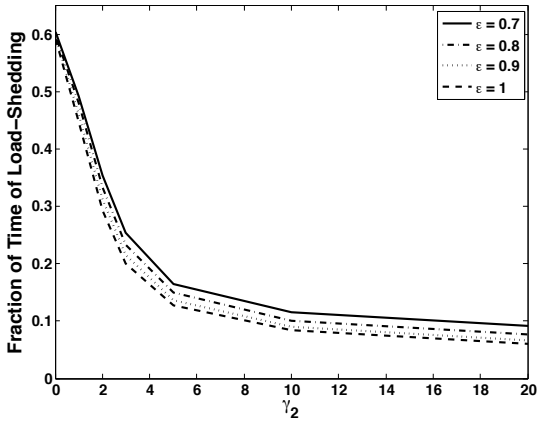

Fig. 12. The effect of varying efficiency ε of storage as a function of γ_2 on the long-term expected fraction of time spent at a load-shedding state for fixed values of $\gamma_1 = 10^4$ and $B = 3$ MWh.

amount of initial storage with $B = 20$MWh, $\gamma_1 = 10^4$, $\gamma_2 = 1$, and $T = 24$ hours for varying values of ε where $\varepsilon_i = \varepsilon_o = \sqrt{\varepsilon}$ (obtained by repeating the analysis of section III.A with the dynamics in (5)). Note that the amount of initial storage at which the transition in the probability of load-shedding from high to low values happens increases with decreasing efficiency.

Figure 12 shows the effect of variations in storage efficiency on the long-term expected fraction of time spent at a load-shedding state as a function of γ_2 for fixed $\gamma_1 = 10^4$ and $B = 3$ MWh. A similar trend is observed for increasing γ_1 with fixed γ_2. Note that, for fixed γ_1, γ_2, and B, a decrease in the storage efficiency leads to an increase in the expected fraction of time at load-shedding.

VI. Discussion

We now discuss how the results presented in the previous section can be translated into design choices. To this end, consider the four configurations corresponding to the crosses in Figure 13 for fixed storage capacity $B = 20$ MWh. Table I shows the area of PV cells and number of wind turbines

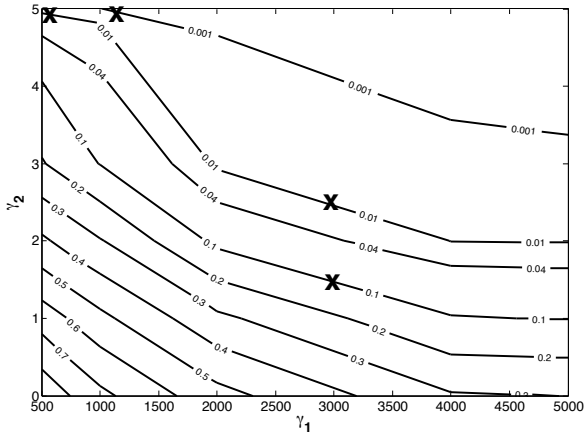

Fig. 13. The long-term expected fraction of time spent at a load-shedding state as a function of γ_1 and γ_2 for a fixed value of storage capacity $B = 20$ MWh.

needed to guarantee specified levels of long-term expected fraction of time at load-shedding. Finally Table II provides the volume of three different storage systems that are capable of supplying $B = 20$ MWh [6], [16].

TABLE I

Area of PV cells and number of wind turbines for specified long-term expected fraction of time at load-shedding

FOT	area of PV cells	number of wind turbines
0.1	$105 \cdot 10^3$ m^2 (25.9 acres)	2
0.01	$105 \cdot 10^3$ m^2 (25.9 acres)	3
0.01	$17.5 \cdot 10^3$ m^2 (4.3 acres)	5
0.001	$38.5 \cdot 10^3$ m^2 (9.5 acres)	5

TABLE II

Volume of different storage options with $B = 20$ MWh

Type of storage	Energy density $[kWh/m^3]$	Volume $[m^3]$
Pumped-hydro (100m of altitude)	0.28	$\sim 5 \times 117 \times 117$ $\sim 41 \times 41 \times 41$
Compressed air	4.17	$\sim 17 \times 17 \times 17$
Lithium-ion battery	300	$\sim 4.1 \times 4.1 \times 4.1$

VII. Conclusions and future work

Motivated by the challenges associated with integration of renewable energy resources in to the electric grid due to source intermittency, we considered a case study on an island off the coast of Southern California, Santa Catalina Island, and investigated the feasibility of replacing diesel generation entirely with solar photovoltaics (PV) and wind turbines, supplemented with energy storage. We used a simple storage model alongside a combination of renewables and varying load-shedding characterizations to determine the appropriate number of PV cells, wind turbines, and energy storage capacity necessary to remain below a certain threshold probability for load-shedding over a pre-specified

period of time and long-term expected fraction of time at load-shedding. Present work focuses on the validation the results using more complicated storage models and load-shedding characterizations as well as data with smaller time increments. Neglected in this paper, but a natural extension of this work is the incorporation of the effects of transmission and distribution.

ACKNOWLEDGEMENTS

This work is partially supported by Southern California Edison (SCE), the Boeing Corporation, and the National Science Foundation. The authors wish to thank Rui Huang for the generating the demand profiles using SAM.

REFERENCES

[1] "2008 Annual Report," Catalina Island Conservancy, Avalon, CA, Tech. Rep., 2008. [Online]. Available: http://www.catalinaconservancy.org
[2] Southern California Edison. [Online]. Available: http://www.sce.com/
[3] C. Archer and M. Jacobson, "Evaluation of global wind power," *Journal of Geophysical Research*, vol. 110, 2005.
[4] T. Ackerman, Ed., *Wind Power in Power Systems*. Wiley, 2005.
[5] "EPRI-DOE Handbook of Energy Storage for Transmission and Distribution Applications," EPRI-DOE, Washington, DC, Tech. Rep., December 2003. [Online]. Available: http://www.sandia.gov/ess/Publications/pubs.html
[6] J. W. Tester, E. M. Drake, M. J. Driscoll, M. W. Golay, and W. A. Peters, *Sustainable Energy: Choosing Among Options*. MIT Press, 2005.
[7] C. Abbey and G. Joos, "A stochastic optimization approach to rating of energy storage systems in wind-diesel isolated grids," *Power Systems, IEEE Transactions on*, vol. 24, no. 1, pp. 418–426, 2009.
[8] A. R. Prasad and E. Natarajan, "Optimization of integrated photovoltaic-wind power generation systems with battery storage," *Energy*, vol. 31, no. 12, pp. 1943 – 1954, 2006.
[9] J. Kaldellis and D. Zafirakis, "Optimum energy storage techniques for the improvement of renewable energy sources-based electricity generation economic efficiency," *Energy*, vol. 32, no. 12, pp. 2295 – 2305, 2007.
[10] J. Barton and D. Infield, "Energy storage and its use with intermittent renewable energy," *Energy Conversion, IEEE Transactions on*, vol. 19, no. 2, pp. 441 – 448, 2004.
[11] P. Lundsager and E. Baring-Gould, "Isolated systems with wind power," in *Wind Power in Power Systems*, T. Ackermann, Ed. Wiley, pp. 299–329.
[12] H. Holttinen and R. Hirvonen, "Power system requirements for wind power," in *Wind Power in Power Systems*, T. Ackermann, Ed. Wiley, pp. 143–167.
[13] M. D. Ilic, J. R. Arce, Y. T. Yoon, and E. M. Fumagalli, "Assessing reliability as the electric power industry restructures," *The Electricity Journal*, vol. 14, no. 2, pp. 55–67, 2001.
[14] J. Norris, *Markov Chains*. Cambridge University Press, 1997.
[15] P. Bremaud, *Markov Chains: Gibbs Fields, MC Simulation, and Queues*. Springer, 1998.
[16] S. M. Schoenung, J. M. Eyer, J. J. Iannucci, and S. A. Horgan, "Energy storage for a competitive power market," *Annual Review of Energy and the Environment*, vol. 21, no. 1, pp. 347–370, 1996.